Insular cortex representation of dynamic mechanical allodynia in trigeminal neuropathic rats

Pedro Alvarez, Wisam Dieb, Aziz Hafidi, Daniel L Voisin, Radhouane Dallel

Neurobiology of Disease 33 (2009) 89–95

Contents lists available at ScienceDirect

Neurobiology of Disease

journal homepage: www.elsevier.com/locate/ynbdi

Insular cortex representation of dynamic mechanical allodynia in trigeminal neuropathic rats

Pedro Alvarez [a,b], Wisam Dieb [a,b,1], Aziz Hafidi [a], Daniel L. Voisin [d,e], Radhouane Dallel [a,b,c,*]

[a] Inserm, U929, Clermont-Ferrand, F-63000 France
[b] Université Clermont1, Clermont-Ferrand, F-63000 France
[c] CHU Clermont-Ferrand, Clermont-Ferrand, F-63000 France
[d] Inserm U862, Neurocentre Magendie, Bordeaux, F-33077 France
[e] Université de Bordeaux, Bordeaux, F-33076 France

ARTICLE INFO

Article history:
Received 3 July 2008
Revised 25 August 2008
Accepted 14 September 2008
Available online 25 September 2008

Keywords:
Nerve injury
Extracellular-signal regulated kinase
Pain
Plasticity

ABSTRACT

Dynamic mechanical allodynia is a widespread symptom of neuropathic pain for which mechanisms are still poorly understood. The present study investigated the organization of dynamic mechanical allodynia processing in the rat insular cortex after chronic constriction injury to the infraorbital nerve (IoN-CCI). Two weeks after unilateral IoN-CCI, rats showed a dramatic bilateral trigeminal dynamic mechanical allodynia. Light, moving stroking of the infraorbital skin resulted in strong, bilateral upregulation of extracellular-signal regulated kinase phosphorylation (pERK-1/2) in the insular cortex of IoN-CCI animals but not sham rats, in whose levels were similar to those of unstimulated IoN-CCI rats. pERK-1/2 was located in neuronal cells only. Stimulus-evoked pERK-1/2 immunopositive cell bodies displayed rostrocaudal gradient and layer selective distribution in the insula, being predominant in the rostral insula and in layers II–III of the dysgranular and to a lesser extent, of the agranular insular cortex. In layers II–III of the rostral dysgranular insular cortex, intense pERK also extended into distal dendrites, up to layer I. These results demonstrate that trigeminal nerve injury induces a significant alteration in the insular cortex processing of tactile stimuli and suggest that ERK phosphorylation contributes to the mechanisms underlying abnormal pain perception under this condition.

Introduction

Neuropathic pain is due to lesion or dysfunction of the peripheral or central nervous system, which generates and maintains abnormal, increased neuronal sensitivity (Woolf and Mannion, 1999). It presents a major therapeutic challenge to healthcare professionals since it is one of the most difficult syndromes to treat successfully (Scholz and Woolf, 2002). Dynamic mechanical allodynia or pain evoked by gentle brushing of the skin is an important characteristic of neuropathic pain. During dynamic mechanical allodynia, activation of the sensory fibers which normally detect touch elicits pain (Ochoa and Yarnitsky, 1993; Koltzenburg et al., 1994; Campbell et al., 1988). From this sensory input, various mechanisms of dynamic mechanical allodynia have been described, that may take place in the dorsal horn (Miraucourt et al., 2007) and along the different brainstem and thalamic relays of pain signal. In addition, previous human imaging studies have revealed a network of brain regions involved in the processing of allodynic pain, including the insula (Moisset and Bouhassira, 2007). Animal studies, however, remain necessary if we want to grasp how higher brain centers contribute to pain perception.

The insula is an integration site for sensations we receive from our bodies such as temperature, hunger, thirst, air hunger and also pain (Craig, 2002; Frot et al., 2006). Imaging studies of clinical allodynia in neuropathic pain consistently demonstrated activation in insula, either ipsi- or bilaterally (Peyron et al., 1998; Becerra et al., 2006; Hofbauer et al., 2006; Schweinhardt et al., 2006; Witting et al., 2006). Discrepancies with other studies (Petrovic et al., 1999; Ducreux et al., 2006) are likely due to methodological differences and to the fact that patient groups investigated vary considerably, regarding symptoms, etiology and levels of ongoing pain. Studies in animals, including electrophysiological recordings in rats (Hanamori et al., 1998; Ito 1998) and monkeys (Robinson and Burton 1980; Dostrovsky and Craig 1996; Zhang et al., 1999), metabolic activity (Porro et al., 1999) and Fos expression (Kuroda et al., 1995; Ter Horst et al., 2001; Wei et al., 2001; Lei et al., 2004) studies, also implicated the insular cortex in acute as well as inflammatory nociception. Furthermore, the insula has been involved in the descending pain modulatory system (Burkey et al., 1996, 1999; Jasmin et al., 2003). To date however, little is known about the insular cortex processing of tactile stimuli in animal models of neuropathic pain.

In the present study we investigated the organization of dynamic mechanical allodynia processing in the rat insular cortex after chronic

* Corresponding author. Inserm U929 Neurobiologie de la douleur trigéminale, Faculté de Chirurgie Dentaire, 11 boulevard Charles de Gaulle, 63000 Clermont-Ferrand, France. Fax: +33 4 73 17 73 06.
E-mail address: radhouane.dallel@u-clermont1.fr (R. Dallel).
[1] Supported by a research study grant from Syrian Government.
Available online on ScienceDirect (www.sciencedirect.com).

0969-9961/$ – see front matter © 2008 Elsevier Inc. All rights reserved.
doi:10.1016/j.nbd.2008.09.003

constriction injury to the infraorbital nerve (IoN-CCI). In the first step, we measured dynamic mechanical allodynia in freely moving rats. In the second step, we quantified extracellular signal-regulated kinase (ERK) phosphorylation in the insula, as a marker of nociceptive processing (Ji et al., 1999). The selective anatomical topography of ERK phosphorylation was also assessed and related to previous findings in human imaging studies.

Materials and methods

Animals

Adult male Sprague–Dawley rats (160–180 g) were obtained from Charles River (L'Arbresle, France) and maintained in a controlled environment (lights on 08:00–20:00, 22 °C) with food and water freely available. They were housed 3–4 per cage. All efforts were made to minimize the number of animals used. The experiments followed the ethical guidelines of the International Association for the Study of Pain and the European Community Council directive of 24 November 1986 (86/609/EEC). All experimental procedures were approved by the local institutional animal care and use committee (UFR d'Odontologie, Université d'Auvergne-Clermont 1).

Chemicals

Unless specifically stated, all chemicals were obtained from Fluka (Germany).

Surgery

Chronic constriction injury of the rat's infraorbital nerve (IoN-CCI) was performed following a previously established surgical procedure (Vos et al., 1994). Briefly, after animals were anesthetized using chloral hydrate (400 mg/kg i.p.), the right IoN was exposed just caudal to the vibrissal pad and two ligatures (4/0 chromic catgut) were loosely tied around the nerve just cranial to its exit from the infraorbital foramen. The ligatures were separated by a 1 mm interval. This procedure was performed under 16 × surgical microscope magnification (Jenoptik, Germany) to allow for the control of the degree of nerve constriction. The nerve diameter was only slightly reduced and ligatures diminished, but did not occlude circulation through the superficial vasculature. Skin incision was closed with single suture points (4/0 nylon). The right IoN of sham animals was similarly exposed but not tied.

Behavioral testing

Rats were tested for dynamic mechanical allodynia only and not for thermal and mechanical hyperalgesia, cold and static allodynia. They were adapted to the observation field and red light for 30 min each day for 3 days prior to the beginning of behavioral testing. During this period, the experimenter reached into the cage to apply gentle air puffing on the face of the animal (see below). For each behavioral testing, rats were placed in the observation field (14×22×16 cm) under red light for a 30-minute period. Gentle air puffing was applied every 3 min perpendicularly to the center of the vibrissal pad (IoN territory). Air-puff stimulus consisted in a jet of about 0.5 s of duration that was manually delivered with a rubber bulb syringe. Stimulation was carried out when the rat was in a sniffing/no locomotion state: with four paws placed on the ground, neither moving nor freezing. The distance to the target from which the stimulus was applied varied from 2 to 5 cm. The tip of the pump was moved towards the target from behind the animal so that it could not see it. Both vibrissal regions were explored in an alternate manner. Each series of stimulation consisted of 10 air puffs applied every 5 s.

The behavioral responses were observed and quantified by a second experimenter according to the method developed by Vos et al. (1994). A rat's response to mechanical stimulation consisted of one or more of the following elements: (1) detection, rat turn head toward stimulus; (2) withdrawal reaction, rat pull paw away or turn head away or pull it briskly backward when stimulation is applied (a withdrawal reaction is assumed to include a detection element preceding the head withdrawal and therefore consists of two responses elements); (3) escape/attack, rats avoid further contact with the stimulus, either passively by moving their bodies away from the stimulus, or actively by attacking the tip of the pump; (4) asymmetric grooming, rats display an uninterrupted series of at least three wash strokes directed to the stimulated area.

The following rank-ordered descriptive response categories were formulated according to the study by Vos et al. (1994): no response, non aversive response, mild aversive response, strong aversive response, prolonged aversive behavior. Each category was given a score (0–4) based on the number of observed response elements. The score was assumed to reflect the magnitude of the aversiveness evoked by the mechanical stimulation (Vos et al., 1994). Score was equal to zero in case of absence of response. A mean score value was then calculated for each stimulation series.

All rats were submitted to 3 sessions of behavioral testing at different time points: before surgery (day 1) and after surgery, on days 7 and 14. These time points were chosen based on a previous study (Vos et al., 1994) that showed decreased responsiveness at around day 7 after surgery, followed by enhanced nociceptive behavior at day 14.

Immunocytochemistry

After the last behavioral testing session at post-operative day 14, IoN-CCI and sham rats were deeply anesthetized with IP urethane (1.5 g/kg) as previously described (Voisin et al., 2005). One hour after the induction of anesthesia, 4 IoN-CCI and 4 sham rats were stimulated for 2 min onto the ipsilateral infraorbital region by gentle air puffing (120 stimuli delivered at 1 Hz), whereas the 4 other IoN-CCI animals did not receive any stimulation. IoN-CCI rats were randomly assigned to one of the two IoN-CCI groups (stimulated and unstimulated).

Two minutes after the end of the stimulation, rats were perfused transcardially with warm (37 °C) heparinized saline (25 IU heparin/ml) followed by cold (10 °C) phosphate-buffered solution (0.1 M, pH 7.6) containing 4% paraformaldehyde and 0.03% picric acid for 15 min.

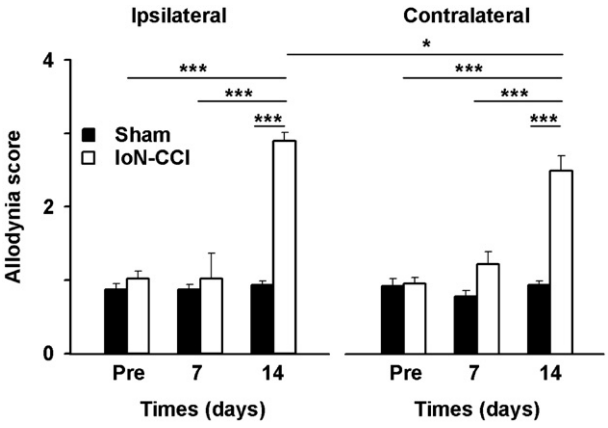

Fig. 1. Infraorbital nerve ligation induces dynamic mechanical allodynia. Bar histogram illustrating the changes in behavioral responses (mean ± SEM) evoked by dynamic tactile mechanical stimulation (air puff) of the ipsilateral and the contralateral face in sham operated rats ($n=4$) and in rats with chronic constriction injury of the infraorbital nerve (IoN-CCI, $n=8$) over two weeks. Only statistically significant differences between allodynia scores are indicated. *$P<0.05$, ***$P<0.001$.

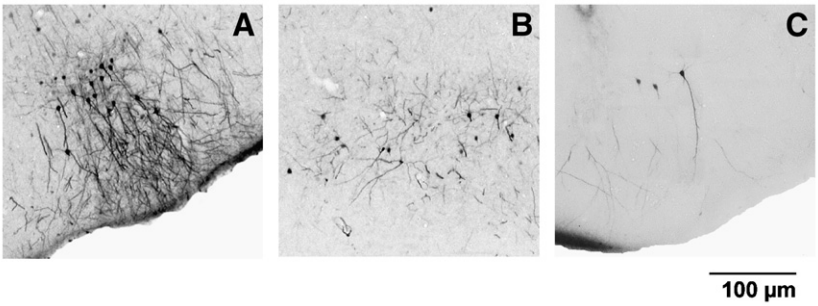

Fig. 2. pERK1/2 in the insular cortex after infraorbital nerve ligation. Images of pERK1/2 immunopositive cell bodies and dendrites in the insular cortex. In (A) and (B) ERK1/2 phosphorylation was evoked by light, dynamic mechanical facial stimuli. (A) Dysgranular insular cortex of an IoN-CCI stimulated rat. (B) Agranular insular cortex of an IoN-CCI stimulated rat. (C) Dysgranular insular cortex of an IoN-CCI unstimulated rat. Bar is 100 µm.

The brain was then removed and transferred in the same paraformaldehyde-picric acid solution containing 30% sucrose at 4 °C and left overnight. Coronal 30 µm thick sections of the forebrain were cut on a freezing microtome (Leica, Germany) and collected in a 0.05 M Tris-buffered saline (TBS).

Free-floating tissue sections were pre-treated in TBS-methanol and 0.3% hydrogen peroxide for 5 min. After 3 washes in TBS, floating sections were incubated in 2% normal horse serum (NHS) in TBS – 0.25% bovine serum albumin – 0.3% Triton X 100 (TBS-BSA-TX) for 30 min, then incubated with mouse anti-pERK-1/2 antibody (1:2000, Cell Signaling Technology, USA) in 1% NHS for 48 h at 4 °C with gentle agitation. After 3 washes in TBS the sections were incubated in a secondary anti-mouse IgG-peroxydase complex (1:4, ImmPRESS® Reagent, Vector, USA) in 1% NHS for 60 min. Following 3 rinses in TBS, immunoreactivity to pERK-1/2 was revealed using a solution containing a phosphate buffer, 3,3′-diaminobenzidine (DAB), nickel chloride and H_2O_2 (DAB Substrate kit, Vector, USA) for 2–10 min. The sections were finally rinsed in TBS, mounted onto gelatin-coated slides, dehydrated in alcohols, cleared in xylene, and coverslipped with DPX. To confirm the localization of pERK-1/2 immunoreactivity, a subset of sections was counterstained with neutral red. As a control for the specificity of the immunostaining procedure, some sections were incubated in 2% NHS without primary antisera. No specific staining was observed in these sections.

To characterize the population of pERK-1/2 immunopositive cells, double immunofluorescence labeling for pERK-1/2 and the neuronal marker NeuN was performed in one set of stimulated IoN-CCI rat brain slices. Briefly, floating sections were incubated in a combination of rabbit anti-pERK-1/2 antibody (1:1000, Cell Signaling Technologies, USA) and mouse anti-NeuN antibody (1:500, AbCys, France) diluted in 2% normal goat serum (NGS)-TBS-BSA-TX 100. Sections were incubated for 48 h at 4 °C. For secondary antibody processing, sections were rinsed 3 times in TBS, and then placed in Cy2 goat anti-rabbit (1:200, Jackson Immunoresearch, USA) and Cy3 goat anti-mouse (1:200, Jackson Immunoresearch, USA) in 2% NGS-TBS-BSA-TX 100 for 120 min at room temperature. After incubation sections were rinsed in TBS, mounted onto gelatin-coated slides and left to dry in a dark environment. Sections were then dehydrated in alcohols cleared in xylene, and coverslipped with DPX.

Data analysis

Bright-field images of single DAB-nickel immunostaining were obtained using a digital camera (Hamamatsu C4742-95, Japan) attached to a Zeiss Axioplan 2 imaging (Germany) microscope, running under MetaMorph v 6.2 software. Dual immunolabeling fluorescence images were captured using an Olympus FV 300 confocal microscope (Japan), each image being made by the assembling of several z-series captured in 1 µm steps. The digital images of Cy2 fluorophore emission were superimposed on identical coordinate images of Cy3 fluorophore emission, allowing double labeling for pERK-1/2 and NeuN. All images were processed for publication in Adobe Photoshop v 5.5 (USA).

Labeled cells were located and counted according to their location in the different layers and divisions of the insular cortex from nine different sections, each taken at a given rostrocaudal plane within the insula, between −0.6 and +2.6 mm from bregma. Intervals of 400 µm between planes ensured that cells were counted only once. The delineation of the insula was based upon the Paxinos and Watson (1997) atlas and the Swanson (1998) atlas.

The rat insular cortex is generally defined as a region overlying the claustrum and that is bounded rostrodorsally by the lateral frontal cortex and the primary somatosensory cortex, caudodorsally by the secondary somatosensory cortex, ventrally by the piriform cortex and caudally by the perirhinal cortex. Although the anatomic criteria to delineate the insular cortex divisions is still a matter of debate, the nomenclature proposed by Cechetto and Saper (1987) remains one of the most widely accepted. According to these authors, the granular insular cortex is the most dorsal insular region that lays immediately ventral to primary and secondary somatosensory cortex. It is characterized by a well-developed granular IV layer. Ventral to the granular insular cortex is an intermediate strip of dysgranular insular cortex in which granule cells of layer IV are markedly diminished in numbers and layer V is more prominent. The dysgranular insular

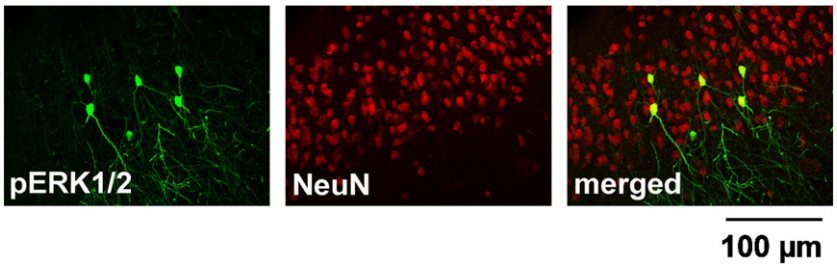

Fig. 3. pERK1/2 is selectively induced in insular cortex neurons. Fluorescence images of pERK-1/2 immunopositive cells (green) and NeuN positive neurons (red) in the insular cortex. ERK1/2 phosphorylation was evoked by light, dynamic mechanical facial stimuli in an IoN-CCI rat. The merged image on the right shows that virtually all pERK-1/2 cells (green) were immunoreactive for NeuN (red), indicating that pERK-1/2 expression was restricted to neurons. Bar is 100 µm.

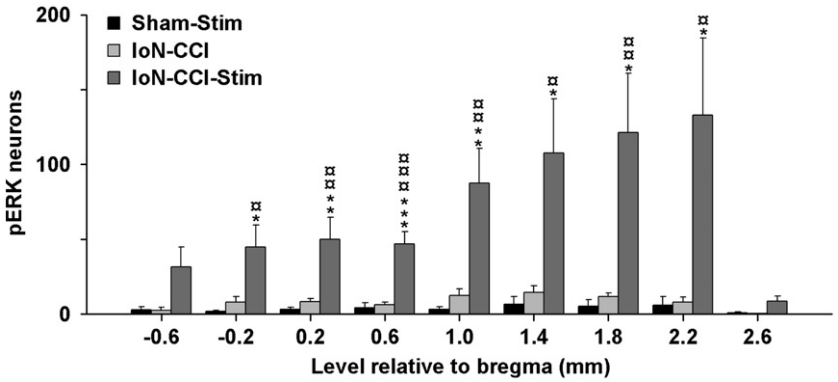

Fig. 4. Stimulus-evoked pERK-1/2 immunopositive cell bodies in IoN-CCI rats predominate in the rostral insula. Bar histogram illustrating the rostrocaudal distribution of pERK-1/2 immunopositive neurons in both sides of the insular cortex between −0.6 mm and +2.6 mm from bregma. In each case, counts are given as mean±SEM (n=4/group). * refers to comparisons between IoN-CCI stimulated rats and sham (*P<0.05, **P<0.01, ***P<0.001) and ¤ refers to comparisons between IoN-CCI stimulated and IoN-CCI unstimulated rats (¤P<0.05, ¤¤P<0.01, ***P<0.001).

cortex extends rostrally to the granular insular cortex and is found ventrally to the lateral frontal cortex. Finally, the agranular insular cortex is the most ventral region and it is located primarily in the groove of the rhinal fissure. It extends rostrally into the rostral portion of the frontal pole and is characterized by three prominent cell layers which are layers II–III, V and VI. Its ventral border marks the end of the four-layer transitional cortex, which becomes the three-layered piriform cortex. The granular insular, dysgranular insular and agranular insular cortices end caudally at the rostral perirhinal cortex.

Statistical analysis

To assess potential differences between groups, one-way analysis of variance (ANOVA) followed by Student–Newman–Keuls test were

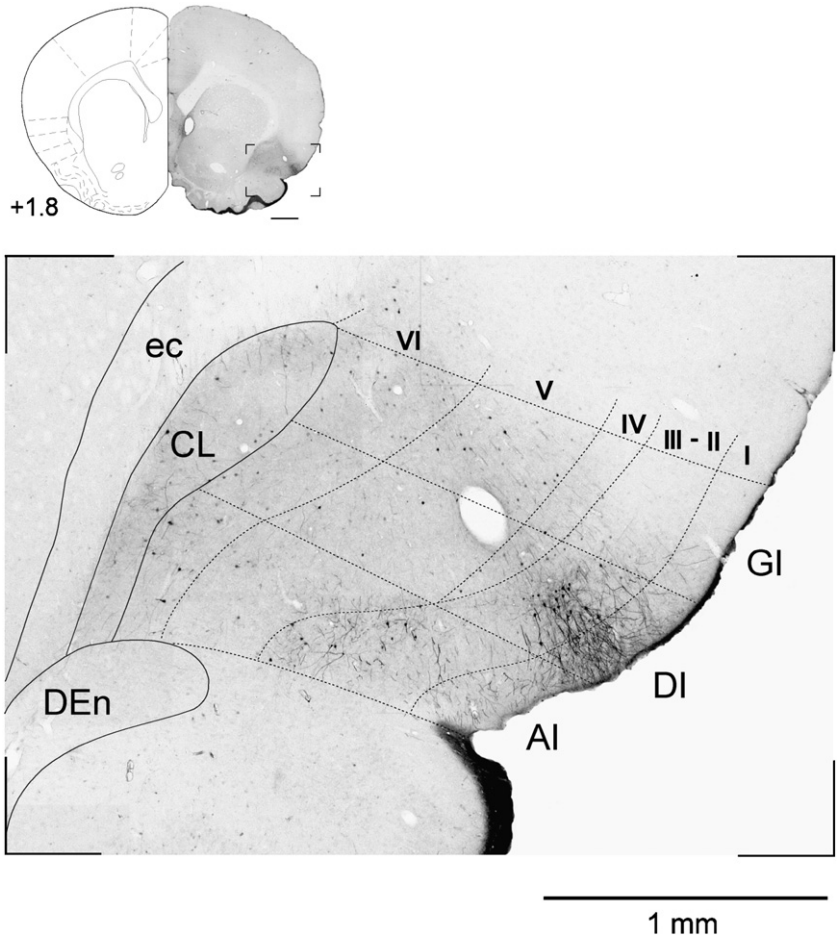

Fig. 5. Layer-selective distribution of pERK1/2 in the insular cortex. Image of a coronal section of the contralateral insular cortex of an IoN-CCI stimulated rat illustrating the distribution of pERK1/2 immunopositive cell bodies and dendrites. pERK-1/2 immunopositive cell bodies were most abundant in layers II–III of the dysgranular and agranular insular cortex. In the dysgranular insular cortex, intense pERK also extended into distal dendrites, up to layer I. The top image shows the location of the insular cortex on a brain coronal section (+1.8 mm from bregma). AI: agranular insular cortex, CL: claustrum, DEn: dorsal endopiriform nucleus, DI: dysgranular insular cortex, ec: external capsula, GI: granular insular cortex. Bar is 1 mm.

performed. Changes in postoperative measurements over time were analyzed with repeated measurement ANOVA. Paired t tests were used for comparison between the ipsilateral and the contralateral side. Results are expressed as mean±SEM. Differences were considered significant at $P<0.05$.

Results

Infraorbital ligation induces dynamic mechanical allodynia

Infraorbital ligation produced a severe ipsilateral face allodynia at post-operative day 14, with the mean score reaching 2.9±0.1 ($n=8$) on a scale ranging from 0 to 4 (Fig. 1). At that time, allodynia was also present on the contralateral side although the contralateral mean score (2.5±0.2) was significantly lower than the ispsilateral mean score (Fig. 1). On both sides scores were significantly higher than preoperative scores and than those in sham animals at post-operative day 14 ($n=4$), IoN-CCI and sham rats at post-operative day 7 (Fig. 1). Scores in sham animals at post-operative day 14, IoN-CCI and sham rats at post-operative day 7 and preoperative scores were not significantly different. Importantly, score values obtained in pre-operative rats (0.9±0.1) confirmed that the mechanical stimuli used in the study were innocuous.

Light, dynamic, mechanical facial stimuli induce pERK-1/2 in the insular cortex after infraorbital ligation

After infraorbital nerve ligation, light, dynamic mechanical facial stimuli induced strong pERK1/2 in the insular cortex on both sides in all individual animals (Figs. 2A, B). There was no significant difference between the numbers of pERK1/2 immunopositive cells in the ipsilateral (304±113) and the contralateral (328±99 cells) insular cortex. These numbers were significantly higher than those found in stimulated sham animals (17±12 and 16±12 respectively, $P<0.05$ in both cases) and unstimulated IoN-CCI rats (39±11 and 32±12 respectively, $P<0.01$ in both cases, Fig. 2C). Numbers in the ipsilateral and contralateral insular cortex of stimulated sham animals and unstimulated IoN-CCI rats were not significantly different.

pERK-1/2 is selectively induced in insular cortex neurons

To characterize the population of pERK-1/2 immunopositive cells, double immunofluorescence labeling for pERK-1/2 and the neuronal marker NeuN was performed in stimulated IoN-CCI rat brain slices. As shown in Fig. 3, virtually all pERK-1/2 immunopositive cells were also immunoreactive for NeuN, which demonstrates that pERK-1/2 was selectively induced in insular cortex neurons.

pERK-1/2 immunopositive neurons are selectively distributed in the insular cortex

As shown in Fig. 4, stimulus-evoked pERK-1/2 immunopositive cell bodies in IoN-CCI rats displayed a rostrocaudal gradient in both sides of the insula, being predominant in the rostral insula (+1.4 mm to +2.2 from bregma). Rostrally, the number of pERK-1/2 immunopositive cell bodies dropped abruptly at +2.6 mm from bregma.

Stimulus-evoked pERK-1/2 immunopositive cell bodies also displayed a layer selective distribution in the insula. Roughly, they were mainly found within the dysgranular and the agranular insular cortex, while only a few ones were observed in the granular insular cortex (Fig. 5 and Table 1).

In the dysgranular insular cortex the highest density of pERK-1/2 immunopositive neurons were found in layers II–III and VI and to a lesser degree in layers IV and V, in all cases with a clear rostrocaudal gradient. Layer I was devoid of cell body and nuclear labeling. However, in the rostral dysgranular insular cortex, an intense immunoreactivity was observed in distal dendrites located in layer I. These dendrites emanated from cell bodies and proximal dendrites situated in layers II–III (Figs. 2A and 5). It is to be noted that in the insular cortex of IoN-CCI unstimulated rats as well as in other parts of the insular cortex of IoN-CCI-stimulated rats, pERK-1/2 immunolabeling was usually limited to the soma and proximal dendrites (Figs. 2A, C).

Table 1
Semi-quantitative assessment of the distribution of pERK-1/2 immunopositive cell bodies in the insular cortex of IoN-CCI stimulated rats

		Level relative to bregma (mm)								
		−0.6	−0.2	0.2	0.6	1	1.4	1.8	2.2	2.6
GI	I	−/−	−/−	−/−	−/−	−/−	−/−	−/−	−/−	−/−
	II–III	−/−	+/−	−/−	−/−	−/−	+/−	+/−	−/−	−/−
	IV	−/−	−/−	−/−	−/−	−/−	−/+	−/−	+/−	−/−
	V	−/−	−/−	−/−	−/−	−/−	−/−	+/+	+/+	−/−
	VI	+/+	+/+	+/−	−/+	+/+	−/++	+/+	+/+	−/−
DI	I	−/−	−/−	−/−	−/−	−/−	−/−	−/−	−/−	−/−
	II–III	−/+	++/+	+/++	+/+	++/++	++/++	+++/+++	+++/+++	+/−
	IV	−/−	+/+	−/+	+/+	+/+	+/++	+/++	+/+	−/−
	V	−/−	+/+	−/+	−/+	+/+	+/++	+/+	++/+	+/+
	VI	+/+	+/++	+/++	+/+	+/++	++/++	+/+	++/++	+/+
AI	I	−/−	−/−	−/−	−/−	−/+	−/−	−/−	−/−	−/−
	II–III	+/+	+/+	+/+	+/+	+/+	++/+	++/++	++/+	+/+
	V	+/+	+/+	+/+	+/−	++/++	+/+	+/+	+/++	−/−
	VI	++/++	++/+	+/++	++/+	++/++	++/++	++/++	+/++	+/−

Estimations are given for the ipsilateral/contralateral sides and relate to the mean cell body counts/slice/rat ($n=4$) as follows: −: <1, +: >1 and <2; ++: 2–10, +++: >10. AI: agranular insular cortex, DI: dysgranular insular cortex; GI: granular insular cortex.

In the agranular insular cortex, the highest densities of pERK-1/2 immunopositive neurons were found all over layer VI. pERK-1/2 immunopositive neurons were also present to a lesser degree in layers V and II–III, with a rostral predominance. Layer I was almost devoid of labeling.

In the granular insular cortex, a few pERK-1/2 immunopositive neurons were found in layer VI and some scattered ones in the layers II to V of the rostral insula.

Discussion

The present study demonstrates for the first time that trigeminal nerve injury induces a significant alteration in the insular cortex processing of tactile stimuli in rats. It also suggests that ERK phosphorylation in insular cortex neurons contributes to the mechanisms underlying abnormal pain perception under this condition. Bilateral ERK phosphorylation was selectively distributed with a rostral predominance within layers II–III and VI of the dysgranular and to a lesser extent, of the agranular insular cortex. In layers II–III of the rostral dysgranular insular cortex, intense pERK also extended into distal dendrites, up to layer I.

Infraorbital ligation induces dynamic mechanical allodynia

Air puffs or air jets have been shown to activate preferentially low threshold Aβ-fibers (Sherman et al., 1997; Miraucourt et al., 2007) and thus are a convenient means of investigating dynamic mechanical allodynia (Ahn et al., 2004; Sherman et al., 1997; Miraucourt et al., 2007). Accordingly, in the present study, naive and sham animals usually exhibited no response or detection behavior only in response to air-puff stimuli. In contrast, after IoN-CCI, air-puff stimuli evoked behaviors that are usually only elicited by nociceptive stimuli, such as vigorous grooming of the stimulation site, vocalization, attempts to escape the stimulus and aggression. The IoN-CCI thus resulted in a disturbance of sensation in which light tactile stimuli appeared to be perceived as highly aversive. The time course of this allodynia was in line with the previously reported mechanical hypersensitivity in the IoN-innervated territory that develops in rats after IoN ligation or

chemically-induced periaxonal inflammation of the IoN (Vos et al., 1994; Idanpaan-Heikkila and Guilbaud, 1999; Benoliel et al., 2002). It was also bilateral, with an ipsilateral predominance, a finding similar to that of Vos et al., (1994), who attributed this to an increased stress level. However, the contralateral changes could also be mediated through brainstem commissural interneurons (Koltzenburg et al., 1999) or created through glial and proinflammatory cytokine action, leading to what has been called a mirror image pain (Milligan et al., 2003). Recent functional imaging work also suggests that the abnormal response to stimulation of the unaffected side could result from cerebral sensitization and involve the insula (Hess et al., 2007)

ERK-1/2 phosphorylation in the insular cortex

ERK signaling pathway plays a crucial role in regulating diverse neuronal processes, such as cell proliferation and differentiation, and long-term synaptic plasticity (Thomas and Huganir, 2004). ERK activation has also been shown to contribute to pain hypersensitivity (Ji et al., 1999). In the spinal and medullary dorsal horn, it is activated by thermal, chemical and mechanical noxious stimuli only, not by stimuli such as light touch or electrical stimulation of Aβ-fibers (Ji et al., 1999). Thus, under normal condition, ERK activation is highly selective for noxious stimulation. Accordingly, we found that in sham rats, air-puff stimuli did not evoke upregulation of pERK-1/2 in neurons of the insular cortex. Rare pERK-1/2 neurons were also observed in the insular cortex of unstimulated IoN-CCI rats. After IoN-CCI, however, innocuous mechanical stimuli induced a dramatic increase in the number of pERK-1/2 immunopositive neurons in both sides of the insular cortex, with a slight but non-significant contralateral dominance. These results show that trigeminal nerve injury induces a significant alteration in the insular cortex processing of tactile stimuli. They are in line with the documented role of the insular cortex in nociception (Craig 2002; Frot et al., 2006) and with the consistent demonstration of insula activation, either ipsi- or bilaterally, by imaging studies of clinical allodynia in neuropathic pain (Peyron et al., 1998; Becerra et al., 2006; Hofbauer et al., 2006; Schweinhardt et al., 2006; Witting et al., 2006). Although the animals showed bilateral allodynia, we did not investigate the effects of stimulation of the contralateral side. It is likely that the insular cortex should be activated by contralateral stimulation too, due to its role in integrating sensations that are received from the body. However, as mentioned above, the insula activation could result from irradiation of the allodynia to the contralateral side across the brainstem, from cerebral sensitization or from both processes (Hess et al., 2007). Whether the same results should apply both qualitatively and quantitatively after contralateral stimulation can thus only be speculated and will require further investigation. Finally, by revealing the involvement of the insular cortex in the processing of dynamic mechanical stimuli after nerve injury and providing a marker of insula activation, our results offer the opportunity to clarify the consequences of action and establish the efficacy of drugs in neuropathic pain.

Selective distribution of neuronal ERK-1/2 phosphorylation in the insular cortex

In this study neuronal pERK-1/2 upregulation predominated in the anterior insular cortex. This is in accordance with PET activation and fMRI studies showing a peak of activation in the rostral portion of the anterior insula in neuropathic pain patients in allodynic condition (Petrovic et al., 1999; Schweinhardt et al., 2006) and also matches the representation of other clinical syndromes reported in the literature review made by Schweinhardt et al. (2006).

Furthermore, disruption of the rostral insular cortex can block the acquisition of external as well as visceral aversively motivated behaviors (Bermudez-Rattoni et al., 1991). Altogether these findings suggest that the rostral insular cortex is involved in the affective-motivational dimension of pain. In contrast, the lower activation of the caudal insular cortex would be related to the autonomic changes resulting from touch-evoked pain (Miraucourt et al., 2007) since most neurons of the caudal insular cortex are activated by baroreceptor stimulation (Cechetto and Saper, 1987) and electrical stimulation of the caudal insular cortex elicits cardiovascular responses (Ruggiero et al., 1987; Sun 1992; Yasui et al., 1991).

Not only ERK phosphorylation displayed a rostral predominance, it was also differentially distributed in the divisions of the insula, being mostly present in the dysgranular insular cortex and to a lesser extent in the agranular insular cortex. Involvement of the agranular insular cortex in nociception, in particular in inflammatory nociception, is well documented (Kuroda et al., 1995; Porro et al., 1999; Wei et al., 2001; Ter Horst et al., 2001; Lei et al., 2004). The agranular insular cortex has also been shown to participate in the descending pain modulatory system (Burkey et al., 1996, 1999). Our data provides the first evidence that in addition to the agranular insular cortex, the dysgranular insular cortex is involved in the processing of brush-evoked allodynia in neuropathic pain rats. Further studies are needed to establish the respective role of each division of the insular cortex in pain processing.

ERK phosphorylation was selectively distributed within layers II–III and VI and to a lesser degree within layers IV–V of the insular cortex. Such a location matches the one of electrophysiologically identified nociceptive neurons in the insular cortex of rats (Hanamori et al., 1998; Ito 1998; Ogawa and Wang, 2002; Wang and Ogawa, 2002) and monkeys (Robinson and Burton 1980; Dostrovsky and Craig 1996; Zhang et al., 1999). Nociceptive specific neurons that respond only to nociceptive stimuli are likely to be found in layers II–III (Ogawa and Wang, 2002; Wang and Ogawa, 2002). Nociceptive non-specific neurons that respond to both nociceptive and non-nociceptive stimuli are mainly located in layer V (Wang and Ogawa, 2002; Ogawa and Wang, 2002). Non-nociceptive, low-threshold mechanoreceptive neurons are found in layers IV and V only (Ogawa and Wang, 2002; Wang and Ogawa, 2002). The present findings thus suggest that after trigeminal nerve injury, innocuous mechanical stimuli could activate previously unresponsive nociceptive neurons in layers II–III of the insular cortex. Accordingly, recent studies have shown in different animal models of neuropathic pain that innocuous stimuli can excite the nociceptive specific neurons of the spinal and medullary dorsal horn (Bester et al., 2000; Torsney and MacDermott, 2006; Miraucourt et al., 2007). Input from these neurons could then reach the insula either through the ascending spino/trigemino-parabrachio-insula pain pathway (Saper 1982; Barnett et al., 1995; Craig, 2002) or through the ventromedial thalamic nucleus (Friedman and Murray, 1986). Additional ERK phosphorylation in layers IV and VI suggests that more than being a simple follower, the insula could also actively contribute to the processing of tactile stimuli in condition of neuropathic pain and thus to the behavioral expression of dynamic mechanical allodynia.

Finally, in layers II–III of the rostral dysgranular insular cortex, intense pERK extended into distal dendrites, up to layer I. A similar extension of pERK expression has been reported in cortical neurons after chronic stress (Trentani et al., 2002) or following visual stimulation *in vivo* (Boggio et al., 2007). Such findings suggest that ERK plays an important role in the local modulation of synaptic function. In the insula, as in the dorsal horn (Ji et al., 1999), this may participate in generating pain hypersensitivity through transcription-dependent and -independent means.

The present study demonstrates for the first time that trigeminal nerve injury induces a significant alteration in the insular cortex processing of tactile stimuli in rats. It also suggests that ERK phosphorylation in insular cortex neurons, more specifically in neurons located in layers II–III and VI of the rostral dysgranular insular cortex, contributes to the mechanisms underlying abnormal pain perception under this condition.

Acknowledgments

We thank AM Gaydier for secretarial assistance. This work was supported by funding from Institut National de la Santé et de la Recherche Médicale (INSERM), Direction Générale des Armées (01.34.012.00470.75.01), Institut Français pour la Recherche Odontologique (IFRO), Fondation Benoit and Université Clermont1 (France).

References

Ahn, D.K., Jung, C.Y., Lee, H.J., Choi, H.S., Ju, J.S., Bae, Y.C., 2004. Peripheral glutamate receptors participate in interleukin-1beta-induced mechanical allodynia in the orofacial area of rats. Neurosci. Lett. 357, 203–206.

Barnett, E.M., Evans, G.D., Sun, N., Perlman, S., Cassell, M.D., 1995. Anterograde tracing of trigeminal afferent pathways from the murine tooth pulp to cortex using herpes simplex virus type 1. J. Neurosci. 15, 2972–2984.

Becerra, L., Morris, S., Bazes, S., Gostic, R., Sherman, S., Gostic, J., Pendse, G., Moulton, E., Scrivani, S., Keith, D., Chizh, B., Borsook, D., 2006. Trigeminal neuropathic pain alters responses in CNS circuits to mechanical (brush) and thermal (cold and heat) stimuli. J. Neurosci. 26, 10646–10657.

Benoliel, R., Wilensky, A., Tal, M., Eliav, E., 2002. Application of a pro-inflammatory agent to the orbital portion of the rat infraorbital nerve induces changes indicative of ongoing trigeminal pain. Pain 99, 567–578.

Bermudez-Rattoni, F., Introini-Collison, I.B., McGaugh, J.L., 1991. Reversible inactivation of the insular cortex by tetrodotoxin produces retrograde and anterograde amnesia for inhibitory avoidance and spatial learning. Proc. Natl. Acad. Sci. U. S. A. 88, 5379–5382.

Bester, H., Beggs, S., Woolf, C.J., 2000. Changes in tactile stimuli-induced behavior and c-Fos expression in the superficial dorsal horn and in parabrachial nuclei after sciatic nerve crush. J. Comp. Neurol. 428, 45–61.

Boggio, E.M., Putignano, E., Sassoè-Pognetto, M., Pizzorusso, T., Giustetto, M., 2007. Visual stimulation activates ERK in synaptic and somatic compartments of rat cortical neurons with parallel kinetics. PLoS ONE 2, e604.

Burkey, A.R., Carstens, E., Jasmin, L., 1999. Dopamine reuptake inhibition in the rostral agranular insular cortex produces antinociception. J. Neurosci. 19, 4169–4177.

Burkey, A.R., Carstens, E., Wenniger, J.J., Tang, J., Jasmin, L., 1996. An opioidergic cortical antinociception triggering site in the agranular insular cortex of the rat that contributes to morphine antinociception. J. Neurosci. 16, 6612–6623.

Campbell, J.N., Raja, S.N., Meyer, R.A., Mackinnon, S.E., 1988. Myelinated afferents signal the hyperalgesia associated with nerve injury. Pain 32, 89–94.

Cechetto, D.F., Saper, C.B., 1987. Evidence for a viscerotopic sensory representation in the cortex and thalamus in the rat. J. Comp. Neurol. 262, 27–45.

Craig, A.D., 2002. How do you feel? Interoception: the sense of the physiological condition of the body. Nat. Rev. Neurosci. 3, 655–666.

Dostrovsky, J.O., Craig, A.D., 1996. Cooling-specific spinothalamic neurons in the monkey. J. Neurophysiol. 76, 3656–3665.

Ducreux, D., Attal, N., Parker, F., Bouhassira, D., 2006. Mechanisms of central neuropathic pain: a combined psychophysical and fMRI study in syringomyelia. Brain 129, 963–976.

Friedman, D.P., Murray, E.A., 1986. Thalamic connectivity of the second somatosensory area and neighboring somatosensory fields of the lateral sulcus of the macaque. J. Comp. Neurol. 252, 348–373.

Frot, M., Magnin, M., Mauguière, F., Garcia-Larrea, L., 2006. Human SII and posterior insula differently encode thermal laser stimuli. Cereb. Cortex. 17, 610–620.

Hanamori, T., Kunitake, T., Kato, K., Kannan, H., 1998. Responses of neurons in the insular cortex to gustatory, visceral, and nociceptive stimuli in rats. J. Neurophysiol. 79, 2535–2545.

Hess, A., Sergejeva, M., Budinsky, L., Zeihofer, H.U., Brune, K., 2007. Imaging of hyperalgesia in rats by functional MRI. Eur. J. Pain 11, 109–119.

Hofbauer, R.K., Olausson, H.W., Bushnell, M.C., 2006. Thermal and tactile sensory deficits and allodynia in a nerve-injured patient: a multimodal psychophysical and functional magnetic resonance imaging study. Clin. J. Pain. 22, 104–108.

Idänpään-Heikkilä, J.J., Guilbaud, G., 1999. Pharmacological studies on a rat model of trigeminal neuropathic pain: baclofen, but not carbamazepine, morphine or tricyclic antidepressants, attenuates the allodynia-like behaviour. Pain 79, 281–289.

Ito, S.I., 1998. Possible representation of somatic pain in the rat insular visceral sensory cortex: a field potential study. Neurosci. Lett. 241, 171–174.

Jasmin, L., Rabkin, S.D., Granato, A., Boudah, A., Ohara, P.T., 2003. Analgesia and hyperalgesia from GABA-mediated modulation of the cerebral cortex. Nature 424, 316–320.

Ji, R.R., Baba, H., Brenner, G.J., Woolf, C.J., 1999. Nociceptive-specific activation of ERK in spinal neurons contributes to pain hypersensitivity. Nat. Neurosci. 2, 1114–1119.

Koltzenburg, M., Torebjork, H.E., Wahren, L.K., 1994. Nociceptor modulated central sensitization causes mechanical hyperalgesia in acute chemogenic and chronic neuropathic pain. Brain 117, 579–591.

Koltzenburg, M., Wall, P.D., McMahon, S.B., 1999. Does the right side know what the left is doing? Trends Neurosci. 22, 122–127.

Kuroda, R., Yorimae, A., Yamada, Y., Nakatani, J., Takatsuji, K., 1995. c-*fos* expression after formalin injection into the face in the cat. Stereotact. Funct. Neurosurg. 6, 152–156.

Lei, L.G., Zhang, Y.Q., Zhao, Z.Q., 2004. Pain-related aversion and Fos expression in the central nervous system in rats. Neuroreport 15, 67–71.

Milligan, E.D., Twining, C., Chacur, M., Biedenkapp, J., O'Connor, K., Poole, S., Tracey, K., Martin, D., Maier, S.F., Watkins, L.R., 2003. Spinal glia and proinflammatory cytokines mediate mirror-image neuropathic pain in rats. J. Neurosci. 23, 1026–1040.

Miraucourt, L.S., Dallel, R., Voisin, D.L., 2007. Glycine inhibitory dysfunction turns touch into pain through PKCgamma interneurons. PLoS ONE 2, e1116.

Moisset, X., Bouhassira, D., 2007. Brain imaging of neuropathic pain. Neuroimage. 37, S80–S88.

Ochoa, J.L., Yarnitsky, D., 1993. Mechanical hyperalgesias in neuropathic pain patients: dynamic and static subtypes. Ann. Neurol. 33, 465–472.

Ogawa, H., Wang, X.D., 2002. Neurons in the cortical taste area receive nociceptive inputs from the whole body as well as the oral cavity in the rat. Neurosci. Lett. 322, 87–90.

Paxinos, G., Watson, C., 1997. The Rat Brain in Stereotaxic Coordinates. Academic Press, New York.

Petrovic, P., Ingvar, M., Stone-Elander, S., Petersson, K.M., Hansson, P.A., 1999. PET activation study of dynamic mechanical allodynia in patients with mononeuropathy. Pain 83, 459–467.

Peyron, R., García-Larrea, L., Grégoire, M.C., Convers, P., Lavenne, F., Veyre, L., Froment, J.C., Mauguière, F., Michel, D., Laurent, B., 1998. Allodynia after lateral-medullary (Wallenberg) infarct. A PET study. Brain 121, 345–356.

Porro, C.A., Cavazzuti, M., Baraldi, P., Giuliani, D., Panerai, A.E., Corazza, R., 1999. CNS pattern of metabolic activity during tonic pain: evidence for modulation by beta-endorphin. Eur. J. Neurosci. 11, 874–878.

Robinson, C.J., Burton, H., 1980. Somatic submodality distribution within the second somatosensory (SII), 7b, retroinsular, postauditory, and granular insular cortical areas of M. fascicularis. J. Comp. Neurol. 192, 93–108.

Ruggiero, D.A., Mraovitch, S., Granata, A.R., Anwar, M., Reis, D.J., 1987. A role of insular cortex in cardiovascular function. J. Comp. Neurol. 257, 189–207.

Saper, C.B., 1982. Convergence of autonomic and limbic connections in the insular cortex of the rat. J. Comp. Neurol. 210, 163–173.

Scholz, J., Woolf, C.J., 2002. Can we conquer pain? Nat. Neurosci. 5, 1062–1067.

Schweinhardt, P., Glynn, C., Brooks, J., McQuay, H., Jack, T., Chessell, I., Bountra, C., Tracey, I., 2006. An fMRI study of cerebral processing of brush-evoked allodynia in neuropathic pain patients. Neuroimage 32, 256–265.

Sherman, S.E., Luo, L., Dostrovsky, J.O., 1997. Altered receptive fields and sensory modalities of rat VPL thalamic neurons during spinal strychnine-induced allodynia. J. Neurophysiol. 78, 2296–2330.

Sun, M.K., 1992. Medullospinal vasomotor neurones mediate hypotension from stimulation of prefrontal cortex. J. Auton. Nerv. Syst. 38, 209–217.

Swanson, L.W., 1998. Brain Maps: Structure of the Rat Brain. Elsevier, New York.

Ter Horst, G.J., Meijler, W.J., Korf, J., Kemper, R.H., 2001. Trigeminal nociception-induced cerebral Fos expression in the conscious rat. Cephalalgia. 21, 963–975.

Thomas, G.M., Huganir, R.L., 2004. MAPK cascade signalling and synaptic plasticity. Nat. Rev. Neurosci. 5, 173–183.

Torsney, C., MacDermott, A.B., 2006. Disinhibition opens the gate to pathological pain signaling in superficial neurokinin 1 receptor-expressing neurons in rat spinal cord. J. Neurosci. 26, 1833–1843.

Trentani, A., Kuipers, S.D., Ter Horst, G.J., Den Boer, J.A., 2002. Selective chronic stress-induced in vivo ERK1/2 hyperphosphorylation in medial prefrontocortical dendrites: implications for stress-related cortical pathology? Eur. J. Neurosci. 15, 1681–1689.

Voisin, D., Guy, N., Chalus, M., Dallel, R., 2005. Noxious stimulation activates locus coeruleus neurones projecting to the somatosensory thalamus in the rat. J. Physiol. Lond. 566, 929–937.

Vos, B.P., Strassman, A.M., Maciewicz, R.J., 1994. Behavioral evidence of trigeminal neuropathic pain following chronic constriction injury to the rat's infraorbital nerve. J. Neurosci. 14, 2708–2723.

Wang, X., Ogawa, H., 2002. Columnar organization of mechanoreceptive neurons in the cortical taste area in the rat. Exp. Brain. Res. 147, 114–123.

Wei, F., Wang, G.D., Kerchner, G.A., Kim, S.J., Xu, H.M., Chen, Z.F., Zhuo, M., 2001. Genetic enhancement of inflammatory pain by forebrain NR2B overexpression. Nat. Neurosci. 4, 164–169.

Witting, N., Kupers, R.C., Svensson, P., Jensen, T.S., 2006. A PET activation study of brush-evoked allodynia in patients with nerve injury pain. Pain. 120, 145–154.

Woolf, C.J., Mannion, R.J., 1999. Neuropathic pain, aetiology: symptoms, mechanisms, and management. Lancet 353, 1959–1964.

Yasui, Y., Breder, C.D., Saper, C.B., Cechetto, D.F., 1991. Autonomic responses and efferent pathways from the insular cortex in the rat. J. Comp. Neurol. 303, 355–374.

Zhang, Z.H., Dougherty, P.M., Oppenheimer, S.M., 1999. Monkey insular cortex neurons respond to baroreceptive and somatosensory convergent inputs. Neuroscience 94, 351–360.